

Image Reconstruction Technology for Voidage Measurement in Two-phase Flow

Qifang Liu^{1,*}, Yan Han², Zhenyu Liu¹ and Huifang Liu³

¹ College of Information Science and Engineering, Shanxi Agricultural University, Taigu030801, China

² National Key Laboratory of Electronic Testing Technology, North University of China, Taiyuan030051, China

³ Faculty of medicine Engineering, University of Hong Kong, Hong Kong

Received 19 September 2015; Accepted 15 November 2015

Abstract

Image reconstruction technology based on electrical resistance tomography (ERT) is one of the most critical voidage measurement techniques in two-phase flow because of the technology's merits, such as visualization, non-intrusiveness, and minimal effect on the environment. However, the reconstruction accuracy of ERT usually presents an enormous challenge because of its ill-posed problems in complexity. A new reconstructed algorithm based on forgetting factor- H_∞ filter (FF- H_∞ filter) for voidage measurement was developed in this study. The H_∞ filter was applied to calculate the filter gain and error matrices for state variable formulation. The forgetting factor was then adaptively adjusted by the residual error of two adjacent times to increase the weight of real-time data and update the status variables with the gain matrix. To reduce the noise information and imaging artifacts, the fuzzy threshold de-noising method was implemented in the data processing. Simulated and practical experiments were combined to contribute to the image reconstruction study. The experiments show that compared with the traditional H_∞ filter, the FF- H_∞ filter can make better use of the three evaluation indexes, improve the reconstructed quality, and significantly reduce boundary artifacts. This method can obtain highly accurate voidage for online measurement because of its strong real-time data availability and anti-jamming capacity.

Keywords: Image reconstruction, FF- H_∞ filter, Voidage measurement, ERT sensor

1. Introduction

Voidage measurement is important in industrial applications and many other scientific fields, such as power management, chemistry, and biotechnology, etc., it is the basis of status monitoring and flow rate and density measurement in two-phase flow [1, 2]. Currently, the voidage values of two-phase flow have been constructed in vertical and horizontal pipes through the use of many effective measurement methods, such as laser technology, data mining, and process tomography [3]. Laser and data mining techniques, such as principal component analysis (PCA), neural network and support vector machine (SVM), etc., require professional facilities and are unsuitable for the demand of visualization environment. The application of process tomography in the voidage measurement of two-phase flow has elicited much attention because of the merits, such as visualization, non-intrusiveness, and minimal influence on the environment. Nevertheless, process tomography presents an ill-posed problem and has thus been studied in recent years; hence, image reconstruction technology remains the focus because of the internal complexity in the reconstruction process [4, 5].

2. Literature Review

Algorithms based on both analytical and iterative methods for electrical tomography are utilized to improve measurement accuracy and reduce the effect of the ill-posed problem for voidage measurement in the electrical resistance tomography (ERT) system. Analytical methods, such as linear back projection (LBP), singular value decomposition (SVD), separable approximation [6], etc., have been widely utilized for low-precision calculation and fast imaging. However, these methods can hardly meet the requirements of reconstruction accuracy. Iterative methods with effective convergence and high image quality, such as total variation regularization [7], conjugate gradient [8], Landweber [9], etc., lack the effectiveness of imaging. Wang Huaxiang et al. reported that the constraint conditions of interference signal are limited as white Gaussian noise; the uncertainty characteristics of the target object are always ignored in both analytical and iterative methods. In fact, determining the dynamic statistical characteristics during the measurement process is difficult. The use of the H_∞ filter is desirable for its strong anti-jamming capacity and robustness in real-time measurement systems; no assumptions are made about the statistical process and measurement noise. This paper presents the initial results of a new reconstruction method for voidage measurement of gas-water flow based on the ERT sensor and H_∞ filter theory. However, the observation data of the current filter are easily obtained from the measured values during the filter progress, which will induce a change in real-time data availability and a filtering error. To solve these problems, a forgetting factor is introduced to adjust the weight of real-time data in the H_∞ filter.

* E-mail address: anq1016@163.com

ISSN: 1791-2377 © 2015 Kavala Institute of Technology.

All rights reserved.

The remainder of the paper is arranged as follows. Section 2 describes the structure of the measurement system and presents the FF-H ∞ filter reconstructed algorithm for voidage measurement as well as the parameter analysis. Section 3 presents the simulation and practical experiment conducted to verify the feasibility and stability of the algorithm. Section 4 provides the conclusions.

3. Methodology

3.1 Voidage measurement system

The voidage measurement system includes an ERT sensor, a switching unit, a data acquisition platform, and a PC. The structure of the ERT system is shown in Fig.2. The data acquisition platform is composed of an resistivity-voltage (R/V) converter, an analog-digital (AD) converter, a digital-analog (DA) converter, a Direct Digital Synthesis (DDS) signal generator, and an ATmega128 microcontroller. The voltages measured in the ERT system are detected to reconstruct medium distributions. The system employs a new sixteen-electrode copper sensor of ERT (Fig.1) to improve the precision of voidage measurement; the copper sensor can obtain 104 measured voltages in the adjacent measurement mode [10, 11]. A new reconstructed algorithm based on the ERT system is introduced to enhance the estimation accuracy in the measurement process.

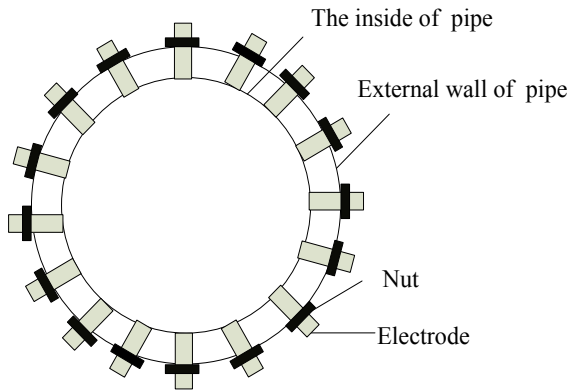


Fig. 1. Electrode structure

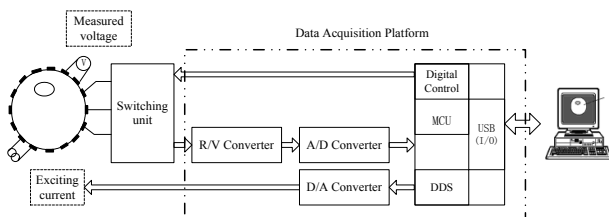


Fig. 2. Schematic of voidage measurement system

The ERT system is utilized to solve two problems. The first problem is to obtain the boundary voltages. Eq. (2) and Eq. (3) provide the boundary conditions. The mathematical model of ERT is defined by the Maxwell equation in Eq. (1).

$$\nabla \cdot (\sigma \cdot \nabla \varphi) = 0, \text{ in } \Omega \tag{1}$$

$$\varphi + z\sigma \frac{\partial \varphi}{\partial n} = V, \text{ in } E_l, l = 1, 2, \dots, L \tag{2}$$

$$\int_{E_l} \sigma \frac{\partial \varphi}{\partial n} = I_l, \text{ in } l = 1, 2, \dots, L \tag{3}$$

Where φ indicates the electrical potential distribution of the sensing field; Z denotes the contact impedances; L is the number of electrodes; E_l and I_l are the electric field strength and injected current in l electrode, respectively; and V is the measurement potentials on the boundary electrodes. Analytical and numerical analyses are employed to solve the boundary problem in the ERT system. However, in the inhomogeneous field, solving the mathematical model by analytical method is a complex task. Numerical analysis method is widely applied in different distribution fields. In this case, the finite element method is selected to address the boundary problem. This method converts the boundary problem into a functional extremum problem based on the variational principle. Then, the field is divided into finite elements, and finite element equations are built on basis of the element information including node number, node coordinate, node potential, and boundary characteristic. Finally, the approximate solution is solved by the numerical method.

The second problem, the reconstruction problem, is called the inverse problem [12]. In this problem, the visualization of field distribution is realized based on the measured voltages. The linear equation for image reconstruction is transformed to

$$V = J \cdot G + e \tag{4}$$

where V and J denote the matrix of the measurement vector and sensitivity coefficients, G is the gray vector matrix, and the measurement error is e . The solution to the inverse problem is to gather the gray vectors by utilizing the measured vector and sensitivity coefficient matrix.

According to the above theory, voidage measurement values are mainly obtained by the pixel distribution. The measured result is provided by

$$\phi = [1 - \sum_{k=1}^m g_k \frac{A_k}{A}] \times 100\% \tag{5}$$

Where, g_k is the gray value of the k pixel, A_k is area of the k pixel, A is total tissue area.

3.2 Reconstructed algorithm based on FF-H ∞ filter

The H ∞ filter estimates the state of the standard linear discrete time system defined as [13]

$$\begin{cases} g_k = g_{k-1} + w_k \\ V_k = J \cdot g_k + v_k \end{cases} \tag{6}$$

Where, J is the sensitive matrix, V_k is the measured boundary voltage. w_k and v_k are called noise terms, which may be random or indeterminacy. The linear combination equation is established to obtain the state estimate at time k in Eq.(7). In Eq.(7), L_k is a full rank matrix. The state estimation of Z_k is called \hat{Z}_k , and the initial state of g is called g_0 . Z_k is solved as a goal. Thus, the following cost function is defined as Eq.(8).

$$\check{Z}_k = L_k \cdot g_k \quad (7)$$

$$\theta_1 = \sup \frac{\sum_{k=0}^{N-1} \left\| Z_k - \check{Z}_k \right\|_{S_k}^2}{\sum_{k=0}^{N-1} (\|w_k\|_{Q_k^{-1}}^2 + \|v_k\|_{R_k^{-1}}^2) + \left\| g_0 - \hat{g}_0 \right\|_{P_0^{-1}}^2} \quad (8)$$

Combined with Eq.(8), the solution to the equation is to obtain an estimation rule to minimize $(Z_k - \check{Z}_k)$ by maximizin θ_1 The new estimation strategy, in which interference level r is investigated in the measurement system, is selected to optimize the threshold. Next, the cost function can be defined as less than $1/r$, as shown in Eq.(9)

$$\theta_1 < 1/r \quad (9)$$

The cost function matrix is applied to Eq.(9) that is in θ to obtain

$$\theta = -1/r \left\| g_0 - \hat{g}_0 \right\|_{P_0^{-1}}^2 + \sum_{k=0}^{N-1} \left[\left\| Z_k - \check{Z}_k \right\|_{S_k}^2 - 1/r (\|w_k\|_{Q_k^{-1}}^2 + \|V_k - J \cdot g_k\|_{R_k^{-1}}^2) \right] < 1 \quad (10)$$

According to the above filter principle, the minimax problem becomes

$$\theta^* = \min_{\hat{g}_k} \max_{V_k, W_k, g_0} \theta \quad (11)$$

Given $\check{Z}_k = L_k \cdot \hat{g}_k$, $v_k = V_k - g_k$, the error norm can be obtained as

$$\|v_k\|_{R_k^{-1}}^2 = \|V_k - J \cdot g_k\|_{R_k^{-1}}^2 \quad (12)$$

$$\left\| Z_k - \check{Z}_k \right\|_{S_k}^2 = (g_k - \hat{g}_k)^T L_k^T S_k L_k (g_k - \hat{g}_k) = \left\| g_k - \hat{g}_k \right\|_{\overline{S}_k}^2 \quad (13)$$

In Eq.(8), Symmetric positive definite matrices such as P_0 , Q_k , R_k , and S_k are selected by the actual measurement based on the specific problem. Meanwhile, S_k should be given. Therefore, \overline{S}_k is defined as

$$\overline{S}_k = L_k^T S_k L_k \quad (14)$$

Substituting the expression for θ into Eq.(15) provides

$$\theta = \psi(g_0) + \sum_{k=0}^{N-1} L_k \quad (15)$$

By simplifying Eq.(15), the expression for status with equations can be summarized as

$$\hat{g}_k = \hat{g}_{k/k-1} + K_k (V_k - J \hat{g}_{k/k-1}) \quad (16)$$

The filter gain and error matrices can be respectively written as

$$K_k = P_{k/k-1} (I - r \overline{S}_k P_{k/k-1} + J^T R_k^{-1} J P_{k/k-1})^{-1} J^T R_k^{-1} \quad (17)$$

$$P_{k/k-1} = P_{k/k-1} (I - r \overline{S}_k P_{k/k-1} + J^T R_k^{-1} J P_{k/k-1})^{-1} + Q_k \quad (18)$$

The H_∞ filter works well but only under the constraint condition in Eq.(19).The range of interference level is limited to $0 < r < r_{\max,k}$ in Eq.(20)

$$P_{k/k-1} (I - r \overline{S}_k P_{k/k-1} + J^T R_k^{-1} J P_{k/k-1})^{-1} > 0 \quad (19)$$

$$r_{\max,k} = \text{Eig}_{\max} (P_{k/k-1}^{-1} + J^T R_k^{-1} J) \quad (20)$$

Where, $r_{\max,k}$ is described as Eq.(20), and Eig_{\max} is the largest eigenvalue of the matrix.

In the following work, forgetting factor β ($\beta > 1$) is introduced in the state iteration equation based on H_∞ filter. According to the filter principle, the iterative procedure can be expressed as

$$\hat{g}_k = \beta \cdot K_k \cdot V_k = (\beta \cdot K_k) \cdot V_k \quad (21)$$

The value of β that provides an adaptive point of the gain matrix can be undated based on the residual error of neighbor time. The equation of adaptive forgetting factor can be computed as

$$\beta_k = [1 - (\|V_{k-1}\|_2 / \|V_k\|_2)] \cdot \tau \quad (22)$$

Where, τ is the adjustment coefficient. If the norm ratio is sufficiently large, the overshoot phenomenon will be generated. This phenomenon has a negative effect on image quality. In addition, directly using the detected data to identify the distribution for reconstructing images is difficult because of the dynamic performance in two-phase flow. To reduce image artifacts in voidage measurement and the reconstruction error, de-noising is conducted. De-noising mainly consists of two steps. First, the noise information is optimized by using smoothing filtering. Second, the pixel units of the reconstructed image are calculated with fuzzy threshold de-noising method [14]. The second step should be completed before reconstructing to obtain better results.

4. Result analysis

Simulated and practical experiments are combined to investigate voidage measurement based on gas-water flow. The measurement voltages are obtained with an ERT array sensor (16 electrodes), and the electrode is simulated by an adjacent measurement model. The three typical distributions are selected to test the proposed algorithm in the

simulations. The models are defined as bubble flow, annular flow, and stratified flow. The assumption is background conductivity and object conductivity are 1S/m and 2S/m, respectively. The reconstructed area is meshed with 576 triangular elements in MATLAB. Three evaluation indexes, namely, peak signal-to-noise ratio (PSNR), root mean squared error (RMSE), and correlation coefficient (CC), are used to evaluate each reconstruction quality as follows [15]:

$$PSNR = 10 \times \log\left(\frac{255^2}{MSE}\right) \tag{23}$$

$$RMSE = \sqrt{\frac{1}{N} \sum_{i=1}^N (\hat{g}_i - g_i)^2} \tag{24}$$

$$CC = \frac{\sum_{i=1}^N (\hat{g}_i - \bar{\hat{g}})(g_i - \bar{g})}{\sqrt{\sum_{i=1}^N (\hat{g}_i - \bar{\hat{g}})^2 \sum_{i=1}^N (g_i - \bar{g})^2}} \tag{25}$$

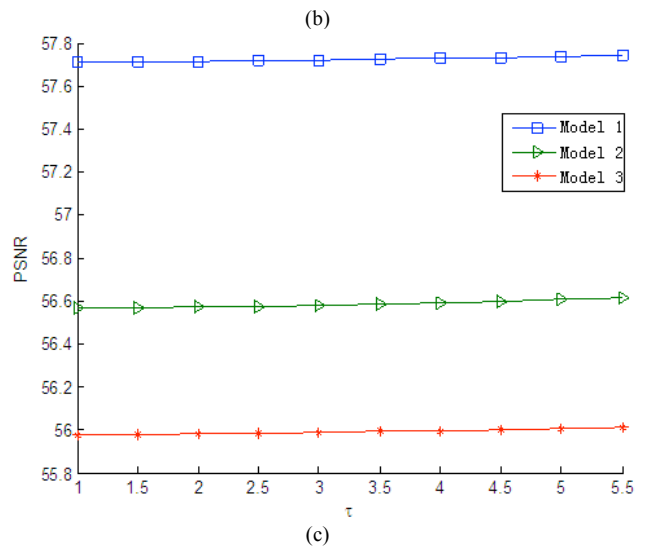
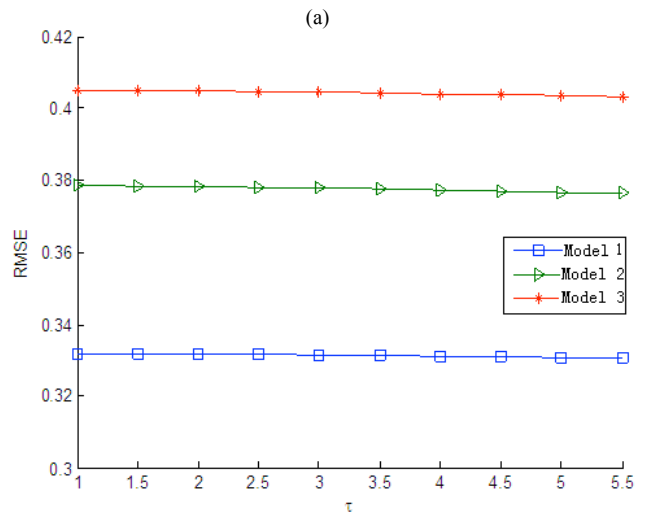
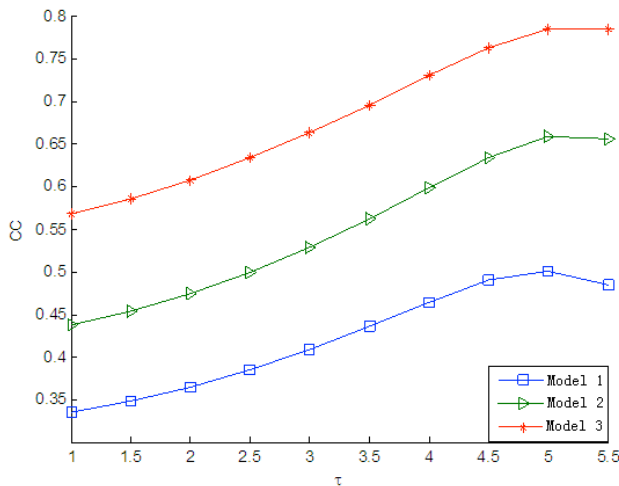
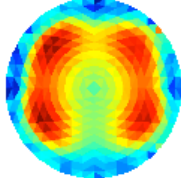
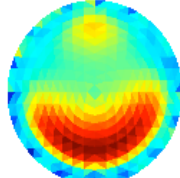
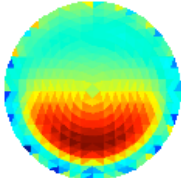


Fig. 3. Plots of influence curve of adjusted parameter τ for reconstruction results. (a) CC results. (b) RMSE results. (c) PSNR results.

Table 1. Reconstruction results of three typical distributions

Method			
H^∞ Filter			

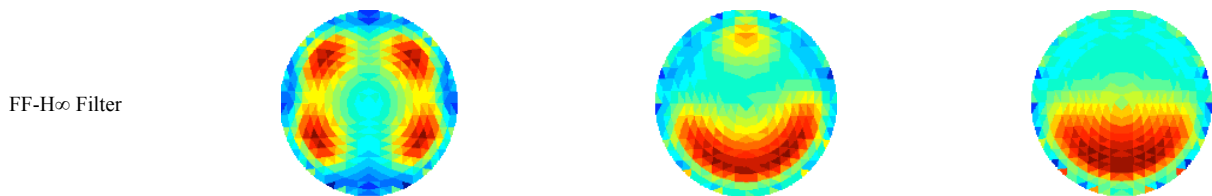


Table 2. Comparison of the evaluate results of different flow patterns

Method/ Flow pattern	H ∞ Filter			FF-H ∞ Filter		
	CC	RMSE	PSNR	CC	RMSE	PSNR
Bubble flow	0.343	0.405	55.266	0.422	0.330	57.76
Annular flow	0.415	0.394	55.076	0.542	0.376	56.625
Stratified flow	0.632	0.436	55.923	0.672	0.401	56.079

In those evaluation formulas, \hat{g}_i is the true pixel distribution of the estimation state, \bar{g} represents an average value of the reconstruction pixel, g_i is the true pixel distribution, and \bar{g} is an average value of the true pixel distribution. MSE denotes the squared error. The larger the absolute values of the correlation coefficient and PSNR are, the better image accuracy is. If RMSE is sufficiently small, then the condition is satisfied with this system. In the FF-H ∞ filter, the forgetting factor is directly introduced to the filter gain matrix to update the state variables. The adjustment coefficient, which includes significant information, is adopted in the filter method. In the next test, the measurement results are obtained by a new strategy of setting different adjusting coefficients. The dynamic error should be ignored for strong robustness of the noise in the H ∞ filter. Fig. 3 shows that in the same constraint condition, the CCs, RMSEs, and PSNRs with different distributions have the same tendency based on the FF-H ∞ filter. When the CCs increase, the RMSEs and PSNRs remain stable for a certain range. Obviously, the distributions can be reconstructed more accurately because of the change in the adjustment coefficient. Thus, many different flow patterns can be tested in the same condition. In fact, confirming the adjustment coefficient based on three evaluation indexes is difficult because the reconstructed values decay and the overshoot phenomenon is generated when the adjustment coefficient is sufficiently large. The coefficient value is set to 3.5.

The reconstructed results of the three typical distributions obtained with the H ∞ filter and FF-H ∞ filter methods are shown in Tables 1 and 2. Comparison of the reconstruction results of the two methods reveals two important points. First, in the measurement results of CCs, the FF-H ∞ filtering method exhibits higher accuracy than the H ∞ filter method. Given that the discrete phase distributions are concentrated, the reconstruction quality of the stratified flow is better than that of bubble and annular flow. Object distribution has a better reconstructed result on basis of the optimized parameters. Second, from the overall performance, the FF-H ∞ filtering model is superior to the H ∞ filtering model in terms of computing. Based on FF-H ∞ filtering theory, the latter can optimize real-time measured voltages and effectively reduces the effects of noise and other prior information under the same prior distribution and noise conditions. Therefore, the proposed filter method not

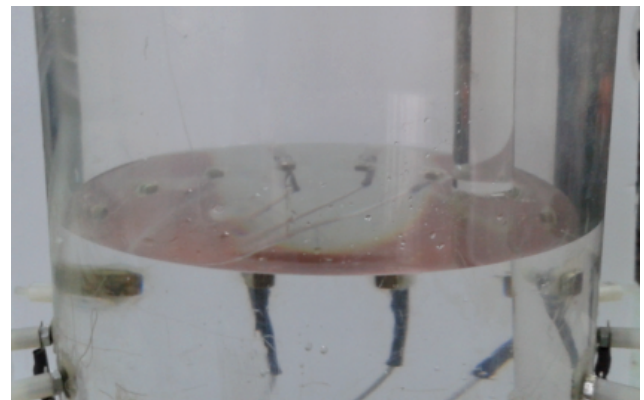
only simplifies the mathematical model of the reconstructing image but also improves the filter accuracy. The FF-H ∞ filtering model obviously has better efficiency and stronger robustness than the H ∞ filtering model in terms of identifying air–water (two-phase) flow patterns.

To further verify the feasibility of the image reconstruction algorithm, a static experiment for gas–water (two-phase) flow is carried out to assess the FF-H ∞ filter method. Water and perspex bars are utilized to simulate the pattern distribution [16]. Perspex bars with different diameters are placed in a pipe with water to simulate different bubble flows. The following three test distributions are created.

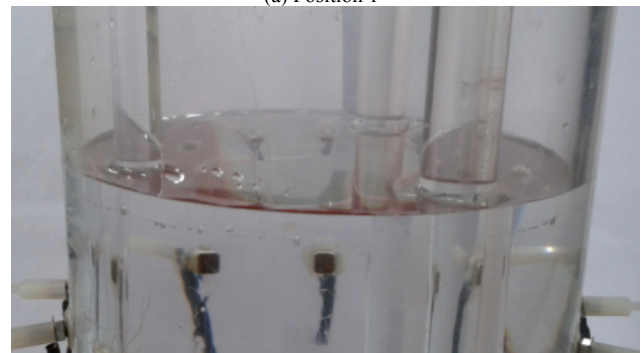
- (a) Position 1: A perspex bar with 18 mm diameter in the 150 mm diameter pipe positioned near the sensor wall
- (b) Position 2: A perspex bar with 12 mm diameter and two glass bars with 18 mm diameter in the 150 mm diameter pipe positioned near the sensor wall
- (c) Position 3: A pipe with 50 mm diameter is placed levelly to simulate stratified flow

To evaluate the voidage measurement results, the maximum relative error is introduced. It is described as

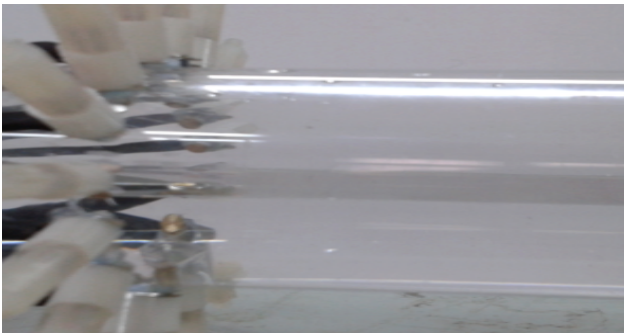
$$E = \left| \frac{\alpha_{mea} - \alpha_{rel}}{\alpha_{rel}} \right| \tag{26}$$



(a) Position 1



(b) Position 2



(c) Position 3

Fig. 4. Diagram of position distribution

Table 3. Compared results of reconstruction image

Method	Position 1	Position 2	Position 3
H_∞ filter			
FF- H_∞ filter			

Table 4. Relative errors of voidage measurement

Method	Position 1	Position 2	Position 3
H_∞ filter	8.11%	12.05%	6.87%
FF- H_∞ filter	7.01%	10.31%	6.06%

The experiments are conducted in a vertical tube pipe and a horizontal pipe. The procedures are shown in Fig. 4. The reconstruction images are obtained from ERT data by the H_∞ filter and FF- H_∞ filter in Table 3. Table 4 shows the relative errors of voidage values during the experiment, which are related to reconstruction accuracy. In the same experimental environment, the test results from subjective and objective aspects are similar to the simulation results. The voidage results from the FF- H_∞ filter are superior to those from the H_∞ filter. The voidage results of stratified flow from voidage measurement in different positions have a smaller error compared with the other methods. Meanwhile, bubble flow has a relatively large error. The error is mainly due to the reconstructed result of position 2, not on other positions, because bubble flow includes many dispersed phases that have a complex relation among the measured voltages. In sum, the test results show that the new method can improve reconstruction quality and enhance the weight of measured voltages compared with the traditional H_∞ filter algorithm.

5. Conclusions

An application of a new robust reconstruction algorithm, established by combining the ERT sensor with the FF- H_∞ filter method to improve imaging in voidage measurement, was presented. Three evaluation indices, namely, CC, RMSE, and PSNR, were used to evaluate the reconstruction quality. Simulation and practical experiments demonstrate that the FF- H_∞ filter performs better in real time than the traditional H_∞ filter; the measurement accuracy of the former is also better than the latter under similar test conditions. Compared with the traditional H_∞ filter, the proposed method has high availability of real-time data and requires minimal computing time. The threshold de-noising method was introduced to reduce the noise information and artifacts in the signal progress; hence, good image resolution was obtained.

The estimation of interference factor is complex in the computation process and has a direct effect on the response time of online measurement. The adaptive interference factor method based on the FF- H_∞ filter will be investigated in the future to improve the computing time and achieve online measurement.

Acknowledgements

This work was supported by the National Natural Science Foundation of China (No. 31371527).

References

1. Mohadeseh Sharifi, B Young. "Electrical resistance tomography (ERT) applications to chemical engineering", *Chemical Engineering Research and Design*, 91(9), 2013, pp.1625-1645.
2. Haifeng Ji, et al., "Voidage measurement of gas-liquid two-phase flow based on capacitively coupled contactless conductivity detection", *Flow Measurement and Instrumentation*, 40, 2014, pp. 199-205.
3. Baoliang WANG, et al. "Voidage Measurement of Air-Water Two-phase Flow Based on ERT Sensor and Data Mining Technology". *Chinese Journal of Chemical Engineering*, 20(2), 2012, pp.400-405.
4. D. Krawczyk-Stando, Rudnicki Marek, "Regularization parameter selection in discrete ill-posed problems—the use of the U-curve", *International Journal of Applied Mathematics & Computer Science*, 17(2), 2007, pp.157–164.
5. Liu QiFang, Yan Han, and XiXiang Zhang. "An image reconstruction algorithm based on Bayesian theorem for electrical resistance tomography", *Optik - International Journal for Light and Electron Optics*, 125(20), 2014, pp.6090-6097.
6. Zhao Jia, Yanbin Xu, Chao Tan, and Feng Dong. "A fast sparse reconstruction algorithm for electrical tomography", *Measurement Science and Technology*, 25(8), 2014, pp.1409-1424.
7. Fan Wenru, Wang Huaxiang and Hao Kuihong. "Two-step iterative TV regularization algorithm for image reconstruction of electrical impedance tomography", *Chinese Journal of Scientific Instrument*, 33(3), 2012, pp.625-630.
8. Qi Wang, Huaxiang Wang, Ziqiang Cui, et al. "Fast reconstruction of electrical resistance tomography (ERT) images based on the projected CG method", *Flow Measurement and Instrumentation*, 27(9), 2012, pp.37-46.
9. Xiao Li-qing, Wang Hua-xiang, Xu Xiao-ju. "Improved landweber algorithm for image reconstruction in electrical resistance tomography system", *Application Research of Computers*, 29(8), 2012, pp.3157-3159.
10. Wang L, Huang Z Y, Wang B L, etc. "Flow pattern identification of gas-liquid two-phase flow based on capacitive coupled contactless conductivity detection", *IEEE Transactions on Instrumentation & Measurement*, 61(5), 2012, pp.1466-1475.
11. Opekar F, Tuma P, Stulik K. "Contactless impedance sensors and their application to flow measurement", *Sensors*, 13(3), 2013, pp. 2786-2801.
12. J. Kaipio, E. Somersalo, "Statistical and Computational Inverse Problems", *Springer-Verlag*, New York, 2005.
13. Simon. "THE H^∞ FILTER, Optimal State Estimation". 2006.
14. Bong SK, AK Khambampati, Sin K, et al. "Image reconstruction with an adaptive threshold technique in electrical resistance tomography", *Measurement Science and Technology*, 22(10), 2011, pp.880-897.
15. Liu Qifang, Han Yan, Zhang Xixiang. "Fast image reconstruction algorithm based on H^∞ filtering for electrical resistance tomography", *Journal of Fiber Bioengineering and Informatics*, 8(1), 2015, pp.125-132.
16. Sharifi Mohadeseh, B Young. "Electrical resistance tomography (ERT) for flow and velocity profile measurement of a single phase liquid in a horizontal pipe", *Chemical Engineering Research and Design*, 91(7), 2013, pp.1235-1244.